

Analysis of deformation coupled surface remodeling in porous biomaterials

Partha Ganguly · Franz-Josef Ulm

Received: 12 December 2006 / Accepted: 20 April 2007 / Published online: 7 August 2007
© Springer Science+Business Media, LLC 2007

Abstract Surface remodeling of biological tissues through tissue growth or dissolution is deemed critical to their proper functioning, and is influenced by the deformation of the tissues during physiological activities. The present work attempts to develop a constitutive framework for deformation modulated surface remodeling of biological tissues. The framework is developed assuming finite deformation of the tissue, and the effect of deformation on the driving force for surface remodeling is determined from thermodynamic principles. The microscopic trends are upscaled to yield the remodeling-induced change in a macroscopic porous tissue. By way of application, the effect of deformation on the remodeling kinetics is determined for an incompressible elastic tissue. Depending on the ratio of the specific elastic stiffness and the specific Gibbs energy variation induced by the cell, the effect of deformation on the remodeling kinetics can be significant. It is found that both tensile and compressive deformation aid tissue dissolution (and dissuade growth). However, the magnitude of the effect is found to be different under tensile and compressive loadings, and critically depends on the reference frame used for the strain measurements. For Lagrangian strain measures (e.g., stretch, engineering strain), the increase in the dissolution kinetics per unit strain is higher under compressive loadings. On the other hand, for Eulerian strain measures (e.g., logarithmic or true strain), the effect of tensile loading on the dissolution

kinetics is higher. This reinforces the need for proper reference frame definition for experimental strain measurements.

Introduction

Many biological tissues continuously undergo remodeling (growth or resorption) during their natural life spans. For example, about 25% of trabecular bone and 3% of cortical bone in a mature adult is remodeled annually. The tissue remodeling phenomena has important consequences, and is deemed critical for a number of physiological events including the healing of bone fracture [1–3], wound healing in the skin [4, 5], hypertrophy of the heart (i.e., size increase in muscles of an overloaded heart, [6]) and changes of pulmonary blood vessels in hypertension [7]. The tissue remodeling mechanism and kinetics are affected by the tissue deformation during the remodeling process, e.g., the contractile forces generated during skin wound contraction is associated with scar tissue formation [8], and the importance of in-vivo stress in bone healing is generally accepted, though the exact nature of the effect is uncertain [1, 9]. Thus modeling of deformation-coupled remodeling processes in biological tissues is important.

The interaction of the remodeling characteristics and the stress/deformation in biological tissues have been numerically examined by several investigators [10–13]. Skalak [10] showed that residual stress may be developed due to non-uniform (and incompatible) growth in biological tissues. Hoger and co-workers [11–13] have modeled deformation coupled growth by introducing a multiplicative split of the total deformation gradient (i.e., due to both

P. Ganguly
Schlumberger Doll Research, Cambridge, MA 02141, USA

F.-J. Ulm (✉)
Massachusetts Institute of Technology, 77 Massachusetts Ave.,
Cambridge, MA 02139, USA
e-mail: ulm@mit.edu

deformation and growth) into its elastic deformation and growth parts, and have analyzed problems related to the hypertrophy of the heart and growth in bones under stress. The analysis is similar to the multiplicative split of the elasto-plastic deformation gradient into the elastic and plastic components in conventional finite deformation elasto-plastic constitutive analysis (e.g., [14, 15]), and estimate the growth phenomenon in terms of its effects on a given set of material points (i.e., the analysis is based on a material reference frame). On the other hand, the remodeling phenomenon involves growth or resorption of the biological tissue, and thus, implicitly involves a change in the number of material points (increase for growth, decrease for resorption), and a continuously variable set of material points. Hoger and co-workers have resolved this anomaly by assuming growth to be volumetric and distributed, i.e., no volume element is destroyed or created during the growth process, rather the existing volume elements are extended or compressed as new material points are added or some material points disappear. Such an approach is effective for volumetric remodeling processes in biological tissues. However, in surface remodeling, the appearance of new material points (or the disappearance of old ones) determine the characteristic of the newly formed surface, and the growth process is spatially discontinuous. Such situations arise in a number of biomaterial remodeling scenarios, including trabecular bone growth/resorption under osteoblast/osteoclast cell action at the bone surface and wound healing in skin tissues (which involve the adhesion of the fibroblast cells at the surface of the skin matrix). The applicability of the multiplicative split in such situations is questionable.

Another characteristic of the trabecular bone/skin remodeling problem deserves mention at this point. Both bone and the skin are porous tissues, composed of struts and pores (see Fig. 1a). The remodeling phenomenon in

these materials can be conveniently divided into two length scales: (a) the microscale (see Fig. 1b), which is typically at the length scale of individual struts or pores for the porous structures, and the relevant scale for biochemical phenomena related to remodeling processes, and (b) the macroscale, which is at the scale length of the entire porous tissue, and is the relevant length scale for determining the effect of remodeling on tissue characteristics. Typically the length scales corresponding to the micro and the macro scale in porous biomaterials differ by one or two orders of magnitude. For example, in porous trabecular bone, the microscale corresponding to the size of individual trabecula and individual pores are of the sizes 100–500 μm [16, 17], while the porous structure, corresponding to the scale of the trabecular bone samples generally used in experiments, is 10–100 mm in size [18]. Similarly, in problems of growth in skin tissues, the length of individual struts and the pore diameter is approximately 100 μm [5], while the scaffolds used in experiments are 1–100 mm in size [5]. It is noteworthy that in both cases, the material addition (or removal) occurs at the lower scale length. The size of the osteoclast cells responsible for resorption in bone is 50 μm [19], while the fibroblast cells involved in skin growth are 20 μm in size [5]. In order to predict the effect of remodeling (which occurs at the microscale) on the macroscopic tissue characteristics, consistent upscaling schemes need to be developed. Such upscaling may be inconvenient when a multiplicative split of the overall deformation gradient is assumed, since the estimation of the macroscopic deformation and growth components of the deformation gradient from the microscopic measurements is not straightforward.

The focus of the present work is the analysis of the remodeling phenomenon (at different length scales) in porous biological tissues. The problem arising from the variability of the material points in such systems is

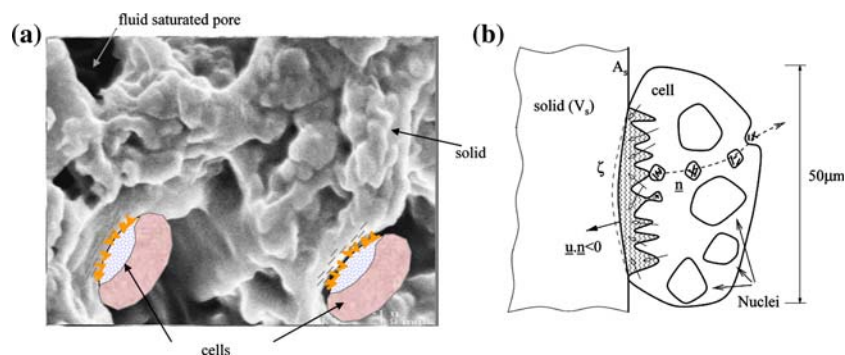


Fig. 1 (a) The porous tissue at the macroscale, consisting of solid struts and fluid saturated pores. The biological cells are shown attached to the solid. (b) Schematic representation of the microscale, where the multinucleated biological cells may attach at the surface of the solid strut, and initiate the remodeling phenomena. The surface

area of the solid strut is A_s , \underline{n} is the normal to the solid surface, the solid-cell interface area is ζ and \underline{u} is the velocity. A negative $\underline{u} \cdot \underline{n}$ at the solid-cell interface signifies dissolution of the solid and a positive $\underline{u} \cdot \underline{n}$ signifies growth

circumvented by developing the theory in terms of a spatial coordinate system. The model is developed both w.r.t. the undeformed reference frame (i.e., at time $t = t_0$), and the deformed (or current) reference frame. The present model follows the analytical lines earlier employed by Silva and Ulm [2] for bone resorption, Lemarchand et al. [20] for mechanically induced dissolution processes, and Ulm et al. [21] for calcium leaching. However, the present work treats the biochemical phenomena at finite strains (whereas infinitesimal strain assumptions were used in the above studies) in order to develop a model for biological tissue remodeling, which may involve small deformations for hard tissues (e.g., bone) and relatively large deformations for soft tissues (e.g., skin).

Remodeling analysis at the microscale

Problem definition

The representative volume element (r.e.v) at this scale contains a solid domain V_s and a cell attached along the cell-solid interface ζ (see Fig. 1b). The mass transfer takes place between the solid surface and the cellular fluid around it, by deposition or dissolution of solid mass from or into the cell fluid. The cell fluid is considered to be a mixture (at pressure p) of a solvent and a solute (partial pressure p_i), generated by the biochemical activity of the cell. The problem is defined in terms of the spatial coordinates, in order to circumvent the difficulty of defining a suitable material coordinate system for a problem with continuous mass (and material points) addition or removal at the cell-solid interface. Since concurrent deformation and growth processes are assumed, the attachment or removal of the material points occur in the deformed solid configuration. Thus, the remodeling problem is initially defined in terms of quantities measured in the deformed configuration (i.e., current reference frame) \underline{x} , and subsequently suitable transformation equations are used to express these quantities in the original (i.e., undeformed) reference frame, \underline{x} .

Figure 2 shows the evolution of several field variables across the solid-cell interface ($x = \zeta$). The solid deforms under the applied loading (external stress and fluid pressure), and simultaneously undergoes mass addition (or removal) at the solid-cell interface, which in turn changes the volume of the solid. In the current configuration, the mass addition (or removal) at the interface may be represented in terms of velocity jump at the solid-cell interface. The particle velocity in the solid bulk (\underline{u}^d) is defined by the microscopic strain rate in the solid, $\underline{d} = \frac{1}{2}(\text{grad}(\underline{u}^d) + \text{grad}^t(\underline{u}^d))$, where $\text{grad}^t(\underline{u}^d)$ is the transpose of the

gradient of the \underline{u}^d vector (i.e., $\text{grad}(\underline{u}^d) = \partial \underline{u}^d / \partial \underline{x}$). This defines the particle velocity at any spatial point inside the solid (approaching the solid-cell interface), and $\underline{u}(\zeta^-) = \underline{u}^d$ (see Fig. 2a). On the other hand, the solid-cell interface velocity is defined by the rate of mass addition to (or removal from) the solid as well as the solid strain rate. Let the velocity component due to the mass addition/removal be \underline{u}^c , defined such that $\underline{u}^c \cdot \underline{n} > 0$ (\underline{n} is the outward normal in the current configuration to the solid-cell interface, see Fig. 2) for addition, and $\underline{u}^c \cdot \underline{n} < 0$ for mass removal. The velocity of the solid-cell interface $\underline{u}(\zeta)$ is defined by the sum of the two components \underline{u}^c and \underline{u}^d , $\underline{u}(\zeta) = \underline{u}^d + \underline{u}^c$. This results in a discontinuity in the velocity field at the solid-cell interface, and the jump in velocity $[[\underline{u}]]$ is defined by

$$[[\underline{u}]] = \underline{u}(\zeta) - \underline{u}(\zeta^-) = \underline{u}^c \tag{1}$$

In case of density, the discontinuity occurs across the solid-cell interface. The solid density at the solid side is defined by solid mass per unit volume $\rho_s(t)$, while that at the cell side is the fluid mass per unit volume, $\rho_f(t)$.

$$[[\rho(t)]] = \rho(\zeta^+, t) - \rho(\zeta^-, t) = \rho_f(t) - \rho_s(t) \tag{2}$$

In the present work, the change in the solid density across the interface is also significant. The solid density jumps from $\rho_s(t)$ on the solid side to 0 in the fluid.

$$[[\rho_s(t)]] = \rho_s(\zeta^+, t) - \rho_s(\zeta^-, t) = -\rho_s(t) \tag{3}$$

Similarly, the jump in the free energy mass-density (free energy per unit mass) across the interface is defined by the difference in the free energy mass-density in the cell fluid (ψ_i) and the solid (ψ_s).

$$[[\psi]] = \psi(\zeta^+) - \psi(\zeta^-) = \psi_i - \psi_s \tag{4}$$

The discontinuities in the density and the free energy mass-density are schematically shown in Figs. 2b and c.

Preliminaries

The focus of the present work is the analysis of deformation coupled remodeling in porous biological tissues, and the analysis is conducted in both the initial (i.e., undeformed) and the current (i.e., deformed) reference frames. The analysis thus involves repeated transformation of quantities between the two reference frames. The equations for volume, density and surface area transformations for a deforming material (without any growth/resorption) are given below.

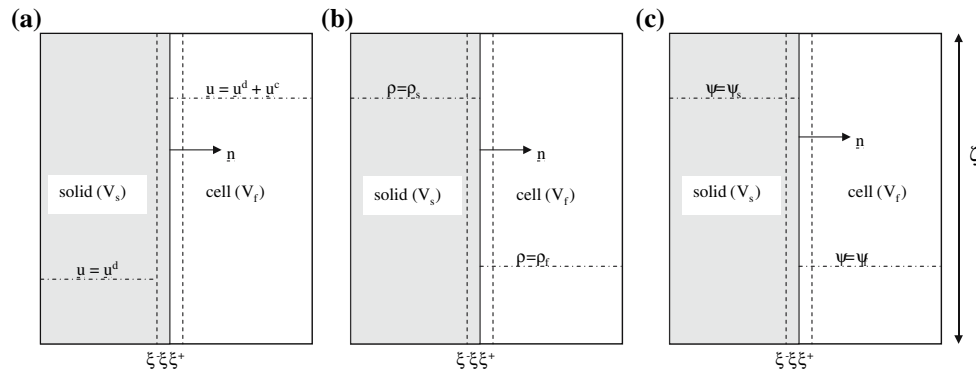


Fig. 2 Schematic representation of the evolution of (a) velocity, (b) density and (c) free energy per unit mass across the solid-cell interface ($x = \zeta$) in the current configuration. The vertical lines corresponding to $x = \zeta^-$ and $x = \zeta^+$ are infinitesimally distant from the interface, and lie in the solid domain (V_s) and the cellular domain (V_c), respectively. The outward normal to the solid-cell interface is

represented by \underline{n} . The area of the solid-cell interface is ζ . The primary purpose of this figure is to show the jump in the field quantities across the solid-cell interface. The field quantities have been shown constant in each of the domains (V_s and V_c) for convenience. No such assumptions have been employed in the analysis

If $v_s(t_0)$ is the original (undeformed) infinitesimal volume of a solid, then the volume $v_s(t)$ after deformation is given by

$$v_s(t) = jv_s(t_0) \tag{5}$$

where, j is the determinant of the deformation gradient f , defined in terms of the undeformed (\underline{X}) and deformed (\underline{X}) reference frames ($f = Grad(\underline{x}) = \partial \underline{x} / \partial \underline{X}$). For a solid with constant mass, the density is inversely proportional to the volume, and the densities in the two reference frames are related by

$$\rho_s(t) = (1/j)\rho_s(t_0) \tag{6}$$

The rate of change of the volume (in terms of quantities in the undeformed configuration) can be expressed by differentiating Eq. (5) w.r.t. time, and realizing that the volume in undeformed configuration $v_s(t_0)$ is independent of time (i.e., $dv_s(t_0)/dt = 0$).

$$\frac{dv_s(t)}{dt} = \frac{dj}{dt}v_s(t_0) \tag{7}$$

If an infinitesimal surface area $da_s(t_0)$ was oriented with an unit normal \underline{n} in the undeformed solid, the corresponding area $da_s(t)$ will be oriented with the unit normal \underline{n} in the deformed solid

$$\underline{n}da_s(t) = j(\underline{f}^{-1})^t \cdot \underline{N}da_s(t_0) \tag{8}$$

where $(\underline{f}^{-1})^t$ is the inverse transpose of the deformation gradient \underline{f} .

Another important concept that is repeatedly applied in the present work is the generalized divergence theorem, which deals with the application of divergence theorem to

fields that exhibit discontinuities within the given domain. For example, if the field $\underline{\omega}$ exhibits a discontinuity at Σ within the domain V of perimeter A , then

$$\int_A \underline{\omega} \cdot \underline{n}_A dA = \int_V div(\underline{\omega})dV + \int_\Sigma [[\underline{\omega}]] \cdot \underline{n}_\Sigma d\Sigma \tag{9}$$

where, \underline{n}_A and \underline{n}_Σ are outward normals at the boundary A and the surface of discontinuity Σ , respectively, and $[[\underline{\omega}]]$ is the jump in the field $\underline{\omega}$ across the surface of discontinuity.

Mass and volume conservation

The mass of solid (considering the solid domain, V_s in Fig. 2) is defined by M_s , and is related to the solid density $\rho_s(t)$ and the solid volume $v_s(t)$ ¹ by

$$M_s(t) = \int_{M_s(t)} dm_s(t) = \int_{V_s(t)} \rho_s(t)dv_s(t) \tag{10}$$

The rate of change of mass is given by

$$\frac{dM_s(t)}{dt} = \int_{V_s(t)} \frac{d\rho_s(t)}{dt} dv_s(t) + \int_{A_s(t)} \rho_s(t)(\underline{u} \cdot \underline{n})da_s(t) \tag{11}$$

where $A_s(t)$ is the area of the solid periphery in the deformed configuration and \underline{n} is the outward normal to the solid periphery. The velocity field \underline{u} is discontinuous in the domain $V_s(t)$ while the density field $\rho_s(t)$ is continuous

¹ In this work, the infinitesimal variables (e.g., $dv_s(t)$) and the integration domains (e.g., $V_s(t)$) have been differentiated through use of different letters or symbols. In some cases, the same symbols have been used to represent the physical quantities at both the micro and the macro-scales.

(see Eq. (1) and Fig. 2). Thus using the generalized divergence theorem (Eq. 9) on the solid domain, the rate of change of the solid mass can be expressed by

$$\frac{dM_s(t)}{dt} = \int_{V_s(t)} \left[\frac{d\rho_s(t)}{dt} + \rho_s(t) \text{div}(\underline{u}^d) \right] dv_s(t) + \int_{\zeta(t)} \rho_s(t) [\underline{u}] \cdot \underline{n} da_c(t) \tag{12}$$

where $\zeta(t)$ is the solid-cell interface area in the deformed configuration (the infinitesimal solid-cell interface area is given by $da_c(t)$) and \underline{n} is the outward normal (outward from the solid) at the interface. The discontinuity of the velocity field $[\underline{u}]$ is defined by \underline{u}^c (see Eq. 1). The above equation contains three terms. The first two terms $d\rho_s(t)/dt$ and $\rho_s(t)\text{div}(\underline{u}^d)$ integrated over the solid volume $v_s(t)$ describe the mass conservation in a deforming solid. The last term defines the mass loss or addition at the solid-cell interface. Considering mass conservation in the solid bulk (i.e., neglecting diffusional mass exchange between the growing/dissolving solid surface and the solid bulk), i.e.,

$$\int_{V_s(t)} \left[\frac{d\rho_s(t)}{dt} + \rho_s(t) \text{div}(\underline{u}^d) \right] dv_s(t) = 0 \tag{13}$$

the mass gain (or loss) is only due to the surface contribution.

$$\frac{dM_s(t)}{dt} = \int_{\zeta(t)} \rho_s(t) \underline{u}^c \cdot \underline{n} da_c(t) \tag{14}$$

Since the rate of mass change is invariant with the change in configuration, the rate in the deformed and undeformed configurations can be equated

$$\frac{dM_s(t)}{dt} = \int_{\zeta(t)} \rho_s(t) \underline{u}^c \cdot \underline{n} da_c(t) = \int_{\zeta(t_0)} \rho_s(t_0) \tilde{\underline{u}}^c \cdot \underline{N} da_c(t_0) \tag{15}$$

where $\rho_s(t_0)$, $\tilde{\underline{u}}^c$ and \underline{N} are the solid density, the velocity of the solid-cell front, and the normal to the solid-cell front, in the undeformed configuration. The growth/dissolution velocities in the undeformed and the deformed configurations may be related by applying Eqs. (6, 8) to Eq. (15).

$$\tilde{\underline{u}}^c = \underline{f}^{-1} \cdot \underline{u}^c \tag{16}$$

The rate of change of the solid volume in the deformed configuration can be derived from Eq. (12) by letting $\rho_s(t) = 1$.

$$\frac{dV_s(t)}{dt} = \int_{V_s(t)} \text{div}(\underline{u}^d) dv_s(t) + \int_{\zeta(t)} \underline{u}^c \cdot \underline{n} da_c(t) \tag{17}$$

The first term reflects the change in volume due to the deformation undergone by the solid, while the second term signifies the corresponding volume increase (or decrease) due to biological growth (or dissolution) at the solid surface. The two activities thus can be clearly demarcated in the deformed configuration. This demarcation is less clear in the undeformed configuration, as evident from the volume change rate derived applying Eqs. (7, 8, 16) to Eq. (17).

$$\frac{dV_s(t)}{dt} = \int_{V_s(t_0)} \frac{dj}{dt} dv_s(t_0) + \int_{\zeta(t_0)} j \tilde{\underline{u}}^c \cdot \underline{N} da_c(t_0) \tag{18}$$

In contrast to Eq. (17), the second term in Eq. (18), reflecting undeformed measures, contains both the biochemical ($\tilde{\underline{u}}^c \cdot \underline{N}$) and the mechanical ($j = \det(\underline{f})$) contributions. The coupling arises due to the fact that Eq. (18) measures the rate of change of current volume (i.e., volume after coupled deformation and mass change) in the undeformed reference frame, and must account for the change in density due to deformation. It may be convenient to introduce the (Lagrangian) mass rate per unit (undeformed) surface involved in the deposition or dissolution process, $\dot{m}^c = \rho_s(t_0) \tilde{\underline{u}}^c \cdot \underline{N}$. Use of \dot{m}^c in Eqs. (15, 18) yield the Lagrangian expressions in the form

$$\frac{dM_s(t)}{dt} = \int_{\zeta(t_0)} \dot{m}^c da_c(t_0) \tag{19}$$

$$\frac{dV_s(t)}{dt} = \int_{V_s(t_0)} \frac{dj}{dt} dv_s(t_0) + \int_{\zeta(t_0)} j \frac{\dot{m}^c}{\rho_s(t_0)} da_c(t_0) \tag{20}$$

Thermodynamic formulation

We are interested in the thermodynamic evolution, in an infinitesimal time interval dt , of a material domain, which at time t coincides with the solid domain $V_s(t)$, and which at time $t + dt$ is composed of the solid domain $V_s(t + dt)$ and of the solute in δV , which corresponds to the solid that dissolved in the cell fluid. These thermodynamic evolutions are subjected to the Clausius-Duhem inequality which states that for all processes the rate of change of Helmholtz free energy (Ψ) is equal to (for reversible processes) or less than (for irreversible) the rate of external work provided to the system (P_{ext}), and results in a non-negative rate of dissipation \mathcal{D} .

$$\mathcal{D} = P_{ext} - \frac{d\Psi}{dt} \geq 0 \tag{21}$$

In the deformed configuration, the external work rate is the sum of two terms. The first term is the work rate developed by the traction field $\underline{t} = \underline{\underline{\sigma}} \cdot \underline{n}$ (with $\underline{\underline{\sigma}}$ the Cauchy stress tensor and \underline{n} the outward normal to the solid surface) and the total solid velocity \underline{u} (composed of velocities due to deformation and chemical growth/dissolution) along the solid surface in the deformed configuration $A_s(t)$

$$P_{ext}(\underline{u}) = \int_{A_s(t)} \underline{u} \cdot \underline{\underline{\sigma}} \cdot \underline{n} da_s(t) = \int_{V_s(t)} \text{div}(\underline{u}^d \cdot \underline{\underline{\sigma}}) dv_s(t) + \int_{\zeta(t)} \underline{u}^c \cdot \underline{n} da_c(t) \tag{22}$$

where the generalized divergence theorem Eq. (9), and Eq. (1) have been used. The last term in Eq. (22) represents the work rate $p\delta V$, involving the fluid pressure p on the boundary of the considered domain and the dissolved solid volume δV , which is obtained by letting $\underline{t} = -p\underline{n}$ in Eq. (22)

$$P_{ext}(\underline{u}) = \int_{V_s(t)} \underline{\underline{\sigma}} : \underline{d} dv_s(t) - \int_{\zeta(t)} p \underline{u}^c \cdot \underline{n} da_c(t) \tag{23}$$

where \underline{d} is the (symmetric) Eulerian strain rate tensor, obtained from developing $\text{div}(\underline{u}^d \cdot \underline{\underline{\sigma}}) = \text{grad}(\underline{u}^d) : \underline{\underline{\sigma}}$, while considering $\text{div} \underline{\underline{\sigma}} = 0$ and $\underline{\underline{\sigma}} = \underline{\underline{\underline{\sigma}}}$ in $V_s(t)$. The second contribution to \mathcal{P}_{ext} of the considered system arises from the introduction (or extraction) of the solute mass dM_i into the cell-fluid, which, given mass conservation of the system under consideration, equals with opposite sign the change in solid mass (given by Eq. 15), i.e., $dM_s/dt = -dM_i/dt = -\rho_i \delta V_i$, where ρ_i is the mass density of the reactant ions in the cell-fluid (assumed for purpose of clarity constant in δV). The resulting work contribution is the work rate $P_{ext}^i = p_i \delta V_i$ developed by the partial pressure of the solute p_i along the rate of change of solute volume $\delta V_i = \int_{\zeta(t)} (\rho_s(t)/\rho_i) \underline{u}^c \cdot \underline{n} d\zeta(t)$. The total external work rate in the deformed reference frame thus reads

$$P_{ext} = P_{ext}(\underline{u}) + P_{ext}^i = \int_{V_s(t)} \underline{\underline{\sigma}} : \underline{d} dv_s(t) - \int_{\zeta(t)} \left(\frac{p}{\rho_s(t)} - \frac{p_i}{\rho_i} \right) \rho_s(t) \underline{u}^c \cdot \underline{n} da_c(t) \tag{24}$$

In the undeformed configuration, the external work terms can be evaluated through suitable transformation of Eq. (24), using Eqs. (6, 8, 15, 19)²

² Using $\text{grad}(\cdot) = \text{Grad}(\cdot) \cdot \underline{f}^{-1}$ and $\underline{\underline{\pi}} = j \underline{\underline{\underline{\sigma}}} \cdot (\underline{f}^{-1})^T$, $\text{div}(\underline{u}^d \cdot \underline{\underline{\sigma}}) = \frac{1}{j} \left[\text{Grad}(\underline{u}^d) \cdot \underline{f}^{-1} \right] : \left[\underline{\underline{\pi}} \cdot \underline{f} \right] = \frac{1}{j} (\underline{f} : \underline{\underline{\pi}})$. Given that $dv_s(t) = j dv_s(t_0)$, $\int_{V_s(t)} \text{div}(\underline{u}^d \cdot \underline{\underline{\sigma}}) dv_s(t) = \int_{V_s(t_0)} (\underline{f} : \underline{\underline{\pi}}) dv_s(t_0)$.

$$\mathcal{P}_{ext} = \int_{V_s(t_0)} (\underline{f} : \underline{\underline{\pi}}) dv_s(t_0) - \int_{\zeta(t_0)} \left(\frac{jP}{\rho_s(t_0)} - \frac{p_i}{\rho_i} \right) \dot{m}^c da_c(t_0) \tag{25}$$

where \underline{f} is the rate of change of the deformation gradient, and $\underline{\underline{\pi}} \equiv j \underline{\underline{\underline{\sigma}}} \cdot (\underline{f}^{-1})^T$ is the Boussinesq (or first Piola-Kirchhoff) stress tensor.

The change of the Helmholtz free energy of the system under consideration is due to the change of the free energy, between t and $t + dt$, in the solid bulk and along the surface of discontinuity. Expressed in terms of the specific free energies, this change in the deformed reference frame is given by

$$\frac{d\Psi}{dt} = \int_{V_s(t)} \rho_s(t) \frac{d\psi_s}{dt} dv_s(t) - \int_{\zeta(t)} (\psi_i - \psi_s) \rho_s(t) \underline{u}^c \cdot \underline{n} da_c(t) \tag{26}$$

where ψ_i and ψ_s are the free energy per unit mass of the solute ions (in the cell fluid) and the solid, respectively. While the first term in Eq. (26) is classical, the second term expresses the spontaneous change at the solid-cell interface, induced by $[[\psi]] = \psi_i - \psi_s$, which can be interpreted as the discontinuity in Eq. (4) in free energy per unit mass between the solute in the cell fluid (ψ_i) and the solid phase (ψ_s). The Lagrangian counterpart of Eq. (26) is readily obtained using Eqs. (5, 6, 15, 19)

$$\frac{d\Psi}{dt} = \int_{V_s(t_0)} \rho_s(t_0) \frac{d\psi_s}{dt} dv_s(t_0) - \int_{\zeta(t_0)} (\psi_i - \psi_s) \dot{m}^c da_c(t_0) \tag{27}$$

Finally, using Eqs. (24, 26) in Eq. (21) yields the Eulerian expression of the dissipation rate

$$\mathcal{D} = \int_{V_s(t)} \left(\underline{\underline{\sigma}} : \underline{d} - \rho_s(t) \frac{d\psi_s}{dt} \right) dv_s(t) + \int_{\zeta(t)} \left[(g_i - \psi_s) - \frac{P}{\rho_s(t)} \right] \rho_s(t) \underline{u}^c \cdot \underline{n} da_c(t) \geq 0 \tag{28}$$

where $g_i = \psi_i + p_i/\rho_i$ is the Gibbs potential or free mass enthalpy (per mass unit) of the solute (ions in the solution of the cell fluid). Analogously, Eqs. (25) and (27) yield the Lagrangian counterpart

$$\mathcal{D} = \int_{V_s(t_0)} \left(\underline{f} : \underline{\underline{\pi}} - \rho_s(t_0) \frac{d\psi_s}{dt} \right) dv_s(t_0) + \int_{\zeta(t_0)} \left[(g_i - \psi_s) - \frac{jP}{\rho_s(t_0)} \right] \dot{m}^c da_c(t_0) \geq 0 \tag{29}$$

The first integral (the volume integral) in these two expressions of the Clausius-Duhem inequality represents the intrinsic dissipation rate in the solid bulk. It is of the standard format classically employed in continuum mechanics. Assuming elastic deformation in the solid bulk, and thus zero dissipation, the terms simply signify that the rate of change of elastic energy in the bulk is governed by the stress–strain work. More generally, in the absence of bio-chemical processes at the solid-cell surface (i.e., $\underline{u}^c \cdot \underline{n} = 0 \Leftrightarrow \dot{m}^c = 0$), it represents the amount of externally supplied energy which is not stored in the solid microstructure, but dissipated into heat form. Given its intrinsic nature, associated with solid deformation, it may be assumed to be non-negative irrespective of the phenomena at the solid-cell surface. Consequently, the dissipation associated with the resorption process which is captured by the surface integrals in Eqs. (28) and (29), must be non-negative as well, i.e.,

$$\varphi_{\zeta(t)} = \left[(g_i - \psi_s) - \frac{p}{\rho_s(t)} \right] \rho_s(t) \underline{u}^c \cdot \underline{n} \geq 0 \tag{30}$$

$$\varphi_{\zeta(t_0)} = \left[(g_i - \psi_s) - \frac{jp}{\rho_s(t_0)} \right] \rho_s(t_0) \tilde{\underline{u}}^c \cdot \tilde{\underline{N}} \geq 0 \tag{31}$$

In contrast to the volumetric dissipation in the solid bulk, the dissipation rate $\varphi_{\zeta(t)}$ is a surface dissipation rate density (of dimension $[\varphi_{\zeta(t)}] = MT^{-3}$). Following standard thermodynamic arguments, expressions Eqs. (30) and (31) may be used to formally identify the term $(g_i - \psi_s) - p/\rho_s(t)$ as the driving force of the influx (in the case of mass deposition) or the outflux (in the case of dissolution) of solid mass per unit surface occupied by cells, which is expressed by $\rho_s(t)\underline{u}^c \cdot \underline{n}$ in the deformed configuration, and $\dot{m}^c(t_0) = \rho_s(t_0)\tilde{\underline{u}}^c \cdot \tilde{\underline{N}}$ in the undeformed configuration. It is convenient to distinguish in ψ_s the energy associated with elastic deformation of the solid from those related to the chemical composition of the solid, by considering $\psi_s = \psi_s^{el} + g_s$, where ψ_s^{el} is the elastic free energy and g_s is the chemical potential per unit solid mass. Furthermore, the dissipation expressions may be rewritten in terms of the molar flux $J = (\rho_s(t)/\mathcal{M})\underline{u}^c \cdot \underline{n}$ in Eq. (30) and $\tilde{J} = (\rho_s(t_0)/\mathcal{M})\tilde{\underline{u}}^c \cdot \tilde{\underline{N}}$ in Eq. (31), where \mathcal{M} is the molar mass, and $\mathcal{M}/\rho_s(t)$ and $\mathcal{M}/\rho_s(t_0)$ the molar volumes of the solid in the deformed and reference configurations

$$\varphi_{\zeta(t)} = \mathcal{A} \times J \geq 0; \quad \varphi_{\zeta(t_0)} = \mathcal{A} \times \tilde{J} \geq 0 \tag{32}$$

where \mathcal{A} is the so-called chemical affinity (see [22, 23]) here of the cell-mediated biochemical reaction.

$$\mathcal{A} = \mathcal{M}(g_i - g_s) - \mathcal{M} \left(\psi_s^{el} + \frac{p}{\rho_s(t)} \right) \tag{33}$$

From Eqs. (30–33) it is apparent that a positive affinity encourages mass addition or surface growth ($u^c = \underline{u}^c \cdot \underline{n} \geq 0$), while a negative driving force encourages mass removal or dissolution at the solid-cell surface ($u^c \leq 0$). This is readily seen for an undeformed solid phase, for which $\varphi_{\zeta(t)} = \varphi_{\zeta(t_0)}$, and for which, following chemical thermodynamics, the first term $\mathcal{M}(g_i - g_s)$ in Eq. (33) is identified as the Gibbs energy variation per mole; that is the difference between the chemical potential of the dissolved ions in the cell fluid, which is controlled by the cell, and which is therefore conveniently referred to as biologically generated potential μ_{BGP} [2], and the chemical potential of the same substance bound in the solid phase μ_s (which in turn is related to the solubility product of the solid). In this case, the chemical affinity coincides with the Gibbs energy variation (see e.g., [24]), i.e., $\mathcal{A}_0 = \mu_{BGP} - \mu_s$. Thus, $(\mu_{BGP} - \mu_s) > 0$ is expected to encourage growth at the solid surface, as evident from the non-negativity of the dissipation. Similarly, for a deformable medium, cellular fluid pressure and/or elastic deformation in the solid will encourage mass dissolution at the solid surface. Adopting the stated link between the Gibbs potential g_i and the biological generated potential μ_{BGP} for constant solute pressure and temperature (for which $g_i = const$), the biochemical affinity becomes

$$\mathcal{A} = \mu_{BGP} - \mu_s - \frac{\mathcal{M}}{\rho_s(t)} (\chi_v^{el} + p) \tag{34}$$

where $\chi_v^{el} = \rho_s(t)\psi_s^{el}$ is the elastic energy per unit current volume, while $\mathcal{M}/\rho_s(t)$ is the current molar volume. Denoting by $\tilde{\chi}_v^{el} = \rho_s(t_0)\psi_s^{el}$ and $\mathcal{M}/\rho_s(t_0)$ the elastic energy per unit volume and the molar volume, respectively, in the undeformed configuration, the driving force can be expressed in Lagrangian variables.

$$\mathcal{A} = \mu_{BGP} - \mu_s - \frac{\mathcal{M}}{\rho_s(t_0)} (\tilde{\chi}_v^{el} + jp) \tag{35}$$

Finally, following standard thermodynamics, the identification of affinity \mathcal{A} as the driving force of the biochemical growth/dissolution at the solid surface, (which qualitatively defines the effect of the different components, e.g., pressure, deformation and biochemical potential difference, on the growth/dissolution tendency at the solid surface) leads to the definition of the kinetics of the growth/dissolution process by a constitutive equation relating the driving force (\mathcal{A}) to the molar flux in the deformed configuration $J = J(\mathcal{A})$, or in the undeformed configuration $\tilde{J} = \tilde{J}(\mathcal{A})$. The simplest form of such a growth/dissolution

law that satisfies the non-negativity of the local dissipation in Eq. (32) is a linear form which captures, similar to a discrete Fick's Law, the diffusion of the ionic species between the solid and the cellular fluid.

$$\mathcal{A} = \left(k \frac{\mathcal{M}}{\rho_s(t)} \right) \underline{J} \equiv \left(\tilde{k} \frac{\mathcal{M}}{\rho_s(t_0)} \right) \tilde{\underline{J}} \quad (36)$$

Or equivalently,

$$\mathcal{A} = ku^c \equiv \tilde{k} \tilde{u}^c \quad (37)$$

where $u^c = \underline{u}^c \cdot \underline{n}$ and $\tilde{u}^c = \tilde{\underline{u}}^c \cdot \underline{N}$. The diffusion coefficient k (of dimension $[k] = LMT^{-1}mole^{-1}$) is primarily governed by the diffusion mechanism in the deformed configuration, and is independent of the factors governing the driving force \mathcal{A} , i.e., pressure, deformation and biochemical potential difference. In return, the diffusion coefficient \tilde{k} in the reference configuration takes into account the change of orientation of the solid surface due to deformation. The two expressions for the diffusion coefficients k and \tilde{k} can be related by using Eqs. (16, 37)

$$\frac{\tilde{k}}{k} = \underline{n} \cdot \underline{f} \cdot \underline{N}^{-1} \quad (38)$$

Finally, it should be noted that surface curvature effects have been neglected in our derivation. The surface curvature affects both the dissolution kinetics, as well as the solid stress state, because of the associated stress discontinuity at the solid-fluid interface (term of the form $\left[\left[\underline{\underline{\sigma}} \right] \right] \cdot \underline{n} = -\gamma \kappa \underline{n}$, where κ is the mean curvature of the solid-cell surface³, and γ is the surface energy per unit area, of dimension MT^{-2}). This stress discontinuity would enter through Eq. (22) the energy derivation, and would ultimately lead to an effect of this curvature term on the dissolution kinetics in a similar way as the fluid pressure. Indeed, it suffices to replace p in Eqs. (34, 35) by an effective pressure $p' = p + \gamma \kappa$. It is no surprise, then, to confirm that a high positive (i.e., outward) curvature of a solid surface leads to a higher dissolution rate, as it has been recognized in skeletal tissue mechanics [25].

Application to porous media

Porosity change

At the microscopic scale, the formulation analyzed deformation coupled remodeling of a single strut of the porous

³ $2\kappa = 1/R_1 + 1/R_2$, with R_1 and R_2 the radius of curvature at the major and minor axis of the solid-cell surface.

biological tissue. At the macroscale, the primary objective is to determine the effects of the remodeling processes (which occurs at the microscale) on variables that are relevant at the scale of the porous material. At this scale, the r.e.v is composed of the solid domain ($V_s(t)$) and the fluid domain ($V_f(t)$), which occupies in the current configuration the volume $V_f(t) = V(t) - V_s(t)$, $V(t)$ being the volume of the porous tissue. The ratio of the current fluid volume over the total initial volume of the r.e.v $V(t_0)$ is referred to as the Lagrangian porosity, and its rate of change is defined as

$$\frac{d\phi}{dt} = \frac{1}{V(t_0)} \left(\frac{dV(t)}{dt} - \frac{dV_s(t)}{dt} \right) \quad (39)$$

Using $V(t) = JV(t_0)$ (where J is the determinant of the macroscopic deformation gradient \underline{F}) and defining $dV_s(t)/dt$ by the upscaled version of Eq. (18), Eq. (39) can be rewritten as

$$\frac{d\phi}{dt} = \frac{1}{V(t_0)} \left(V(t_0) \frac{dJ}{dt} - \int_{V_s(t_0)} \frac{dj}{dt} dv_s(t_0) - \int_{\zeta(t_0)} j \tilde{\underline{u}}^c \cdot \underline{N} da_c(t_0) \right) \quad (40)$$

where $V_s(t_0)$ is now the total solid volume in the porous material, and $\zeta(t_0)$ is the total cell-solid interaction surface (for the entire porous tissue being considered), both expressed in the undeformed configuration. Expressing the volume average of the rate of change of j by $\langle \frac{dj}{dt} \rangle$, i.e., $\int_{V_s(t_0)} \frac{dj}{dt} dv_s(t_0) = V_s(t_0) \langle \frac{dj}{dt} \rangle_{V_s(t_0)}$, Eq. (40) can be reduced to

$$\frac{d\phi}{dt} = \frac{dJ}{dt} - c_s(t_0) \left\langle \frac{dj}{dt} \right\rangle_{V_s(t_0)} - \frac{1}{V(t_0)} \int_{\zeta(t_0)} j \tilde{\underline{u}}^c \cdot \underline{N} da_c(t_0) \quad (41)$$

or equivalently, using the upscaled version of Eq. (20),

$$\frac{d\phi}{dt} = \frac{dJ}{dt} - c_s(t_0) \left\langle \frac{dj}{dt} \right\rangle_{V_s(t_0)} - \frac{1}{V(t_0)} \int_{\zeta(t_0)} j \frac{\dot{m}^c}{\rho_s(t_0)} da_c(t_0) \quad (42)$$

where $c_s(t_0) = V_s(t_0)/V(t_0)$ is the solid volume fraction in the undeformed porous material, and $\dot{m}^c = \rho_s(t_0) \tilde{\underline{u}}^c \cdot \underline{N}$ is the mass rate per unit (undeformed) surface involved in the cell-mediated deposition or dissolution process. The first and second terms in Eqs. (41) and (42) represent the contribution of pure mechanical deformation (the entire porous material and the solid phase, respectively) to the change in porosity, and are the classical terms employed in the Biot-Coussy theory of porous media [22]. The third term signifies the contribution of the biochemical growth/dissolution process, amplified by deformation.

Dissipations

For upscaling of the Clausius-Duhem inequality from the micro-scale of the solid (see Eq. 29) to the macro-scale of the porous continua, the r.e.v in the macro-scale (consisting of the porous tissue, as shown in Fig. 1a) is considered to be subjected at the external boundary $\partial V(t_0)$ to a uniform velocity boundary condition, and at the fluid–solid interface, i.e., along $\partial V_f(t)$, to a uniform pore fluid pressure p . The presentation is inspired by the derivation of Biot’s poromechanics theory by Dormieux et al. [26]. For purpose of analysis, the boundary of the r.e.v $\partial V(t_0)$ is assumed to be located in the solid domain, so that the fluid domain is surrounded by solid. In this case, the boundary conditions read

$$\partial V(t_0) : \underline{u}^d = \underline{\dot{F}} : \underline{X} \tag{43}$$

$$\partial V_f(t) : \underline{t} = -p\underline{n} \tag{44}$$

where $\underline{\dot{F}}$ is the macroscopic deformation gradient rate, \underline{u}^d denotes the microscopic velocity field in the solid phase that leads to deformation, and \underline{n} is the unit normal vector oriented outward with respect to the solid at the fluid–solid interface. The macroscopic counterpart of Eq. (22) then is the sum of two work rate terms provided to the solid phase:

1. The work rate developed by the surface tractions $\underline{\pi} \cdot \underline{N}$ and the velocity \underline{u}^d prescribed on $\partial V(t_0)$ in the reference configuration. Given the uniform boundary condition Eq. (43), this term can be developed with the help of the Hill Lemma (see Appendix)

$$P_{ext}(\underline{u}^d) = \int_{\partial V(t_0)} (\underline{u}^d \cdot \underline{\pi}) \cdot \underline{N}_b da(t_0) = \left(\underline{\dot{F}} : \underline{\Pi} \right) V(t_0) \tag{45}$$

where \underline{N}_b is the unit outward normal vector to $\partial V(t_0)$, and $\underline{\Pi} = \left\langle \underline{\pi} \right\rangle_{V(t_0)}$ is the macroscopic Boussinesq tensor, that is the volume average of the microscopic tensor $\underline{\pi}$ over the total volume of the porous medium $V(t_0)$.

2. The work rate developed by the uniform pore pressure p and the rate of volume change $dV_f/dt = -\int_{\partial V_f(t)} \underline{u} \cdot \underline{n} da(t)$ (composed of the volume change due to deformation and chemical growth/dissolution) along the solid–fluid interface. Since the fluid–surface interface is entirely surrounded by the solid phase, the corresponding volume change equals the change in pore space. Hence, with Eq. (39)

$$p \frac{dV_f}{dt} = p \frac{d\phi}{dt} V(t_0) \tag{46}$$

Finally, if we add to the two contributions, given by Eqs. (45, 46), the additional work rate related to the introduction (or extraction) of the solute mass dM_i into the cell–fluid, we obtain the macroscopic counterpart of Eq. (25).

$$\mathcal{P}_{ext} = V(t_0) \left(\underline{\dot{F}} : \underline{\Pi} + p \frac{d\phi}{dt} \right) + \int_{\zeta(t_0)} \left(\frac{p_i}{\rho_i} \right) \dot{m}^c da_c(t_0) \tag{47}$$

Or equivalently, using Eq. (42), Eq. (47) can be rewritten as

$$\mathcal{P}_{ext} = V(t_0) \left(\underline{\dot{F}} : \underline{\Pi} + p \frac{d\phi^*}{dt} \right) - \int_{\zeta(t_0)} \left(\frac{j p}{\rho_s(t_0)} - \frac{p_i}{\rho_i} \right) \dot{m}^c da_c(t_0) \tag{48}$$

where $d\phi^*/dt$ stands for the change in Lagrangian porosity in the absence of mass addition or removal processes.

$$\frac{d\phi^*}{dt} = \frac{dJ}{dt} - c_s(t_0) \left\langle \frac{dj}{dt} \right\rangle_{V_s(t_0)} \tag{49}$$

Equation (48) expresses the work rate provided to the solid phase. Indeed, it is nothing but an application of Eq. (25) using the boundary conditions given by Eqs. (43, 44). The associated change of the Helmholtz free energy in the solid phase is given by the upscaled version of Eq. (27). Assuming the solid chemical potential (g_s) is invariant with time ($dg_s/dt = 0$), and using Eq. (33), the rate of change of Helmholtz free energy at the macroscopic scale can be rewritten in the form

$$\frac{d\Psi}{dt} = V(t_0) c_s(t_0) \left\langle \frac{d\tilde{\chi}_v^{el}}{dt} \right\rangle_{V_s(t_0)} - \int_{\zeta(t_0)} \left(\frac{\mathcal{A}}{\mathcal{M}} + \frac{j p}{\rho_s(t_0)} - \frac{p_i}{\rho_i} \right) \dot{m}^c da_c(t_0) \tag{50}$$

where $\tilde{\chi}_v^{el}$ is the microscopic elastic energy volume-density, measured in the undeformed configuration. Finally, using Eqs. (48, 50) in Eq. (21) yields the Clausius-Duhem inequality at the macroscopic scale (in the undeformed reference frame)

$$\mathcal{D} = \mathcal{D}_m + \mathcal{D}_c \geq 0 \tag{51}$$

where, \mathcal{D}_m , denoting the rate of dissipation due to mechanical factors, and \mathcal{D}_c , the rate of dissipation primarily due to growth/dissolution (but including the coupled terms), are respectively given by

$$\mathcal{D}_m = V(t_0) \left(\underline{\underline{F}} : \underline{\underline{\Pi}} + p \frac{d\phi^*}{dt} - c_s(t_0) \left\langle \frac{d\tilde{\chi}_v^{el}}{dt} \right\rangle_{V_s(t_0)} \right) \quad (52)$$

$$\mathcal{D}_c = \int_{\zeta(t_0)} \mathcal{A} \left(\frac{\dot{m}^c}{\mathcal{M}} \right) da_c(t_0) \quad (53)$$

Equation (52) is the standard form of the mechanical dissipation associated with the pure (finite) deformation of the solid phase of a porous material, as described by the classical Biot theory. The additional dissipation caused by the biological activity of cells attached to the solid surface is captured by Eq. (53), where \mathcal{A} is the affinity defined in various forms and configurations by Eqs. (33–35): it is the driving force of the mass deposition or dissolution flux \dot{m}^c and of the associated solid growth $\underline{u}^c \cdot \underline{n}$ or $\underline{\tilde{u}}^c \cdot \underline{N}$. Provided the value of the affinity is known, the rate of the biological mediated mass removal can be determined from kinetics laws, such as Eqs. (36, 37), and the resulting change of the porosity and the overall solid behavior can be evaluated.

Example of deformation coupled remodeling

The effect of imposed deformation on the dissolution rate at the surface of a cylindrical strut at the microscale is explored in this section. The surface of the solid strut may be assumed to be smooth and the curvature effect on the dissolution rate is neglected. For an undeformed solid, the growth velocity is u_0^c , the corresponding biochemical affinity is $\mathcal{A}_0 = \mu_{BGP} - \mu_s$, and the solid volume is V_0 . From Eq. (37),

$$\mathcal{A}_0 = k u_0^c \quad (54)$$

The solid subsequently undergoes uniaxial deformation. Assuming the solid (a soft biological tissue) to be an incompressible isotropic Hookean material, the change in the elastic energy density may be written as (following [27])

$$\Delta \tilde{\chi}_v^{el} = \frac{E}{4(1+\nu)} (I_\lambda - 3) \quad (55)$$

where E is the elastic modulus and ν the Poisson's ratio for the isotropic biological tissue, and $I_\lambda = \lambda_1^2 + \lambda_2^2 + \lambda_3^2$, λ_1^2 , λ_2^2 , λ_3^2 being the eigenvalues of the symmetric Cauchy dilatation tensor ($\underline{\underline{C}} = \underline{f}^t \cdot \underline{f}$). Assuming that the fluid pressure (p) and the biochemical potential term ($\mu_{BGP} - \mu_s$) are insensitive to the imposed deformation, the driving force for growth/dissolution in the deformed solid is given by (see Eq. 35)

$$\mathcal{A} = \mathcal{A}_0 - \frac{\mathcal{M}}{\rho_s(t_0)} \tilde{\chi}_v^{el} \quad (56)$$

Normalizing both sides of Eq. (56) by \mathcal{A}_0 , and using Eqs. (37, 54, 55), the dissolution velocities in the deforming and the undeformed solid can be related by

$$u^c = u_0^c \left[1 - \left(\frac{E\mathcal{M}}{\mathcal{A}_0\rho_s(t_0)} \right) \frac{(I_\lambda - 3)}{4(1+\nu)} \right] \quad (57)$$

For uniaxial deformation (in x_1 -direction) of an incompressible tissue, $\nu = 0.5$, and I_λ is given by⁴ $I_\lambda = \lambda_1^2 + 2\lambda_1^{-1}$.

Physically, λ_1 is an eigenvalue of $\sqrt{\underline{\underline{C}}}$ and the stretch of a material element in the uniaxial loading direction. Thus, Eq. (57) can be rewritten in a dimensionless form

$$\frac{u^c}{u_0^c} = 1 - \left(\frac{E\mathcal{M}}{\mathcal{A}_0\rho_s(t_0)} \right) \frac{\lambda_1^2 + 2\lambda_1^{-1} - 3}{6} \quad (58)$$

The dimensionless number $\mathcal{E} = E\mathcal{M}/\mathcal{A}_0\rho_s(t_0)$ is the ratio of the specific elastic modulus of the soft biological tissue ($E/\rho_s(t_0)$) and the specific affinity ($\mathcal{A}_0/\mathcal{M}$) of the biochemical process that takes place at the solid-cell interface, and may be considered as a measure of the relative importance of the elastic deformation vis-a-vis the pure biochemical driving force on the overall remodeling kinetics. Estimation of \mathcal{E} for soft tissues is unavailable to the best of our knowledge. However, \mathcal{E} for dissolution in hard-tissues (bone) may be estimated from the work of Silva and Ulm [2] ($\rho_s(t_0)\mathcal{A}_0/\mathcal{M} \approx -31$ MPa), and Rho et al. [28] ($E \approx 17$ GPa), which yields $\mathcal{E} \approx -548$ for bone dissolution (This value may still be higher if one considers the stiffness of the hydroxyapatite crystals that build up the ultrastructure of bone; see e.g., [17]). Figure 3a shows the normalized dissolution velocities (u^c/u_0^c) for \mathcal{E} values ranging from -1 to $-1,000$, for stretch ratios ranging from 0.5 to 2 (i.e., engineering strains from -0.5 (compression) to $+1.0$ (tension)). It is evident that both compressive and tensile deformation of the solid enhance the dissolution rate, at all \mathcal{E} values. The effects, as expected from Eq. (58), increase with increasing $|\mathcal{E}|$. Quantitatively, the effects of compressive and tensile deformations on the dissolution rate are dissimilar, and the rate of dissolution rate enhancement (per unit stretch or engineering strain) is larger under compressive loading. It should however be noted that the dissolution enhancement effect is relative to the chosen strain measure; here the stretch—a Lagrangian strain measure. This trend is inverted if an Eulerian strain

⁴ For an incompressible solid, the third invariant of the Cauchy dilatation tensor $\lambda_1^2\lambda_2^2\lambda_3^2 = 1$. For uniaxial deformation in an isotropic solid, $\lambda_2 = \lambda_3$. Thus, $\lambda_2^2 = \lambda_3^2 = \lambda_1^{-1}$, and $\lambda_1^2 + \lambda_2^2 + \lambda_3^2 = \lambda_1^2 + 2\lambda_1^{-1}$.

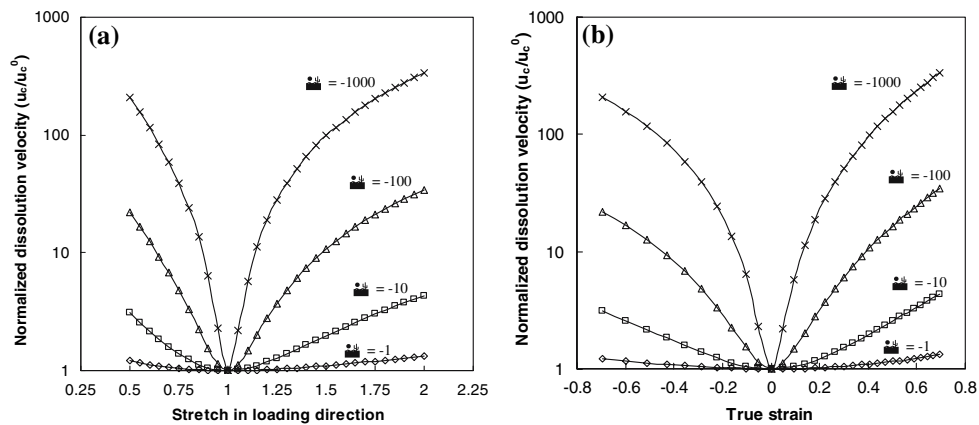


Fig. 3 Representation of the normalized dissolution velocity variation for different soft biological tissues under uniaxial loading, in (a) Lagrangian and (b) Eulerian strain measures. The Lagrangian measure of tissue deformation is defined by the stretch in the loading direction (stretch = (final length)/(initial length)). This signifies compression for stretch <1 and tension for stretch >1. The Eulerian

deformation measure is defined by the true strain in the loading direction (natural log of stretch), signifying compression for negative true strain and tension for positive strain. The tissue properties are characterized by \mathcal{E} , which signifies a ratio of the elastic deformation energy and the biochemical energy for the tissue remodeling (see text)

measure is employed, such as the true (logarithmic) strain which is related to the (Lagrangian) stretch by $\epsilon^{\ln} = \ln(\lambda_1)$. The results displayed in Fig. 3b indicate, for the same value of $|\epsilon^{\ln}|$, a higher dissolution rate enhancement in tension than in compression. This underscores the necessity to specify (both theoretically and experimentally) the reference frame (Lagrangian or Eulerian) used for measuring field quantities.

Conclusion

The present work attempts to develop an integrated analysis for deformation coupled surface remodeling in porous biomaterials. In such materials (examples include trabecular bone and skin), the biochemical phenomenon related to remodeling (growth/dissolution) occurs at a microscopic scale and estimation of its effect on the tissue level (macroscopic) properties is important. In the present work, the remodeling and deformation (at the microscale) in the biological tissues is modeled through development of suitable equations for mass, volume and the relevant thermodynamic quantities for the growing solid, which are then upscaled to yield the macroscopic effects. The equations are developed assuming a spatial reference frame, to circumvent the problems of defining a suitable material reference frame for growth/dissolution processes, characterized by a continuous change in the number of material (and mass) points. The analysis examined the effects of different field quantities on the growth/dissolution potential of the solid-cell interface. A positive pressure of the cellular fluid and deformation of the solid was observed to encourage solid dissolution (and tissue resorption), while

an increase in the chemical potential of the dissolving ions (compared to their potential in the solid) was observed to encourage tissue growth. The microscopic equations were upscaled to yield the tissue characteristics (e.g., change in Lagrangian porosity) at the macroscale. A numerical example on the effect of deformation on the dissolution rate for an incompressible soft tissue showed that the rate increased for both tensile and compressive deformations. The change of the dissolution rate (per unit strain) depended on the strain measure. For Lagrangian measures (e.g., stretch), the rate increase per unit strain was higher under compressive loading than under tensile loading. On the other hand, the rate increase per unit strain was higher under tensile deformation when an Eulerian measure (e.g., true strain) was used.

Acknowledgments The authors wish to thank the Natural Sciences and Engineering Research Council (NSERC) of Canada and the Esther and Harold E. Edgerton Chair at MIT for financial assistance. The authors are thankful to Profs. Lorna Gibson (MIT), Olivier Coussy (Institute de Navier, France), and Luc Dormieux (Institute de Navier, France), and Dr. Anirban Sain (McGill University, Canada) for helpful discussions.

Appendix: Hill Lemma

This demonstration of the Hill Lemma is inspired by the presentation of Zaoui [29]. We denote by $\underline{\underline{\pi}}$ and $\underline{\underline{f}}$ the microscopic Boussinesq tensor which (in the absence of body forces) satisfies $\text{Div} \underline{\underline{\pi}} = 0$ in $V(t_0)$, and the microscopic deformation gradient rate tensor $\underline{\underline{f}} = \text{Grad}(\underline{u})$. If, either $\underline{\underline{f}}$ satisfies a uniform deformation boundary condition, or $\underline{\underline{\pi}}$ a uniform traction boundary condition, then

$$\langle \underline{\dot{f}} : \underline{\pi} \rangle_{V(t_0)} = \langle \underline{\dot{f}} \rangle_{V(t_0)} : \langle \underline{\pi} \rangle_{V(t_0)} = \underline{\dot{F}} : \underline{\Pi} \tag{59}$$

(1) Consider the r.e.v V subjected to a uniform velocity boundary condition

$$\text{on } \partial V(t_0) : \underline{u} = \underline{\dot{F}} \cdot \underline{X} \tag{60}$$

where $\underline{\dot{F}}$ represents the deformation rate of the r.e.v at the macroscopic scale, while \underline{u} is defined at the microscopic scale. The work rate provided to the r.e.v by the surface traction $\underline{t} = \underline{\pi} \cdot \underline{n}$ in the undeformed configuration reads (in components)

$$\mathcal{P} = \int_{\partial V(t_0)} u_i t_i da(t_0) = \dot{F}_{ij} \int_{\partial V(t_0)} X_j \pi_{ik} N_k da(t_0) \tag{61}$$

Application of the divergence theorem yields, for any stress field π_{ik} that satisfies $\pi_{ik,k} = 0$ (that is $\text{Div} \underline{\pi} = 0$) yields

$$\begin{aligned} \int_{\partial V(t_0)} X_j \pi_{ik} N_k da(t_0) &= \int_{V(t_0)} (X_j \pi_{ik})_{,k} dv(t_0) \\ &= \int_{V(t_0)} (\pi_{ik} \delta_{jk} + X_j \pi_{ik,k}) dv(t_0) \\ &= \int_{V(t_0)} \pi_{ij} dv(t_0) \end{aligned} \tag{62}$$

Thus, inputing $\langle \pi_{ij} \rangle_{V(t_0)} = \underline{\Pi}_{ij}$ in Eq. (61)

$$\mathcal{P} = V(t_0) \dot{F}_{ij} \underline{\Pi}_{ij} = V(t_0) \underline{\dot{F}} : \underline{\Pi} \tag{63}$$

(2) Consider the r.e.v subjected to a uniform traction boundary condition

$$\text{on } \partial V(t_0) : \underline{t} = \underline{\pi} \cdot \underline{N} = \underline{\Pi} \cdot \underline{N} \tag{64}$$

where $\underline{\Pi}$ is the macroscopic Boussinesq tensor, while \underline{t} is the microscopic stress vector (defined on the undeformed configuration). The work rate is developed in the form:

$$\mathcal{P} = \int_{\partial V} u_i t_i dA = \int_{\partial V} u_i \pi_{ij} N_j dA = \int_{\partial V} u_i N_j dA \underline{\Pi}_{ij} \tag{65}$$

Application of the divergence theorem yields

$$\begin{aligned} \int_{\partial V} u_i N_j dA &= \int_{\partial V} u_i \delta_{jk} N_k dA = \int_{V(t_0)} (u_i \delta_{jk})_{,k} dV(t_0) \\ &= \int_{V(t_0)} u_{i,k} \delta_{jk} dV(t_0) = \int_{V(t_0)} \dot{f}_{ij} dV(t_0) \end{aligned} \tag{66}$$

Again, inputing $\langle \dot{f}_{ij} \rangle_{V(t_0)} = \dot{F}_{ij}$ in Eq. (65)

$$\mathcal{P} = V(t_0) \dot{F}_{ij} \underline{\Pi}_{ij} = V(t_0) \underline{\dot{F}} : \underline{\Pi} \tag{67}$$

References

1. Cowin SC (1983) *Ann Biomed Eng* 11:263
2. Silva EC, Ulm F-J (2002) In: Karihaloo BL (ed) *Proc. IUTAM Symp. on Analytical and Computational Fracture Mechanics of Non-Homogeneous Materials*, Kluwer Acad. Pub., London, p 355
3. Ballarini R, Kayacan R, Ulm F-J, Belytschko T, Heuer AH (2005) *Int J Fracture* 135(1–4):187
4. Grinnell F (1994) *J Cell Biol* 124:401
5. Freyman TM, Yannas IV, Pek Y-S, Yokoo R, Gibson LJ (2001) *Exp Cell Res* 269:140
6. Lund D, Tomanek RJ (1978) *Am J Anat* 152:141
7. Sobin SS, Tremmer HM, Hardy JD, Chiodi HP (1983) *J Appl Physiol* 55:1445
8. Yannas IV, Lee E, Orgill DP, Skrabut EM, Murphy GF (1989) *Proc Natl Acad Sci USA* 86:933
9. Pauwels F (1980) *Biomechanics of the locomotor apparatus*. Springer-Verlag, Berlin
10. Skalak R (1981) In: Carlson DE, Shield RT (eds) *Proc. IUTAM Symp. on Finite Elasticity*, Martinus Nijhoff, The Hague, p 348
11. Rodriguez EK, Hoger A, McCulloch AD (1994) *J Biomech* 27:455
12. Chen Y-C, Hoger A (2000) *J Elast* 59:175
13. Lubarda VA, Hoger A (2002) *Int J Solids Struct* 39:4627
14. Lee EH (1969) *J Appl Mech* 36:1
15. Lubarda VA (1991) *Int J Solids Struct* 27:885
16. Gibson LJ (1985) *J Biomech* 18:317
17. Hellmich C, Ulm F-J (2002) *J Biomech* 35:1199
18. Zysset PK, Curnier A (1996) *J Biomech* 29:1549
19. Blair HC (1998) *BioEssays* 20:837
20. Lemarchand E, Dormieux L, Ulm F-J (2003) In: Huyghe JM (ed) *Proc. IUTAM Symp. on the Mechanics of Physicochemical and Electromechanical Interactions in Porous Media*, Kerkrade (Netherlands)
21. Ulm F-J, Lemarchand E, Heukamp FH (2003) *Eng Fract Mech* 70:871
22. Coussy O (1995) *Mechanics of porous continua*. J. Wiley & Sons, Chichester UK
23. Coussy O, Ulm F-J (1996) *Arch Appl Mech* 66(8):523
24. Atkins PW (1994) *Physical chemistry*. WH Freeman and Company, New York, p 216
25. Martin RB, Burr DB, Sharkey NA (1998) *Skeletal tissue mechanics*. Springer-Verlag, New York
26. Dormieux L, Djimedo K, Ulm F-J (2006) *Microporomechanics*. J. Wiley & Sons, Chichester UK
27. Attard MM (2003) *Int J Solids and Struct* 40:4563
28. Rho JY, Roy ME, Tsui TY, Pharr GM (1999) *J Biomed Mater Res* 45:48
29. Zaoui A (1997) *Materiaux heterogene et composites (lecture notes, Edition 1997)*. Departement de Mecanique, Ecole Polytechnique, France